Journal of
Synchrotron Radiation

ISSN 0909-0495

Received 26 August 2009
Accepted 14 September 2009

Developing VUV spectroscopy for protein folding and material luminescence on beamline 4B8 at the Beijing Synchrotron Radiation Facility

Ye Tao,* Yan Huang, Zhenghua Gao, Hao Zhuang, Aiyu Zhou, Yinglei Tan, Daowu Li and Shuaishuai Sun

Beijing Synchrotron Radiation Facility (BSRF), Institute of High Energy Physics, Chinese Academy of Sciences, People's Republic of China. E-mail: taoy@ihep.ac.cn

The new 4B8 beamline provides UV–VUV light in the wavelength range from 360 to 120 nm. It uniquely enables two kinds of spectroscopy measurements: synchrotron radiation circular dichroism spectroscopy and VUV excited fluorescence spectroscopy. The former is mainly used in protein secondary structure studies, and the latter in VUV excited luminescent materials research. Remote access to fluorescence measurement has been realised and users can collect data online. Besides steady-state measurements, fluorescence lifetime measurements have been established using the time domain method, while a laser-induced temperature jump is under development for protein folding dynamics using circular dichroism as a probe.

Keywords: VUV spectroscopy; circular dichroism; fluorescence; time-resolved spectroscopy; remote access.

1. Introduction

VUV spectroscopy, with a wavelength range from 200 down to around 120 nm (the cut-off wavelength of the optical window), has attracted special attention because two kinds of spectroscopy in this range are important in biological and materials research. One is circular dichroism (CD) spectroscopy, which measures the absorption difference between circularly left- and right-polarized light in biomolecules. CD is widely used to determine the secondary structure of proteins, and the absorption bands of the peptide bond fall mainly between 250 and 160 nm. Commercial CD spectrometers generally only measure down to 200 nm owing to the low intensity of lamp sources below 200 nm. However, most structure information is contained below 200 nm (Miles & Wallace, 2006). Synchrotron sources can provide intensive light, thus allowing high-quality data to be extended below 200 nm. In addition, synchrotron radiation circular dichroism (SRCD) measurements are usually carried out in solution phase, requiring a very small amount of sample and no limit on macromolecule size. Therefore, SRCD has emerged as a powerful technique for investigating protein structure, and has become an attractive complement to protein crystallography and NMR methods in structural and functional proteomics. Several SRCD beamlines have been constructed and some are under commissioning or planned (Dicko *et al.*, 2004; Clarke & Jones, 2004; Matsuo *et al.*, 2005; Mirona *et al.*, 2005; Sutherland, 2002; Yagi-Watanabe *et al.*, 2007).

The development of VUV (wavelength < 200 nm) excited luminescent materials has been important because these phosphor materials are widely used in mercury-free lamps and panel display devices (Wegh *et al.*, 1999). In these devices an inert gas (Xe or Xe/Ne) discharge emitting between 140 and 190 nm is employed to excite the phosphors. Besides, wide-band semiconductors also require characterization below 200 nm (Sedhain *et al.*, 2008). For the same reason, synchrotron sources play an important role in VUV excited fluorescence spectroscopy. Some synchrotron VUV beamlines for fluorescence spectroscopy are currently operational (Lee *et al.*, 2008; Lin *et al.*, 2007; Zimmerer, 2007).

The interesting range for these two methods falls into the same VUV region (200–120 nm). However, there are few beamlines that meet the requirements of both methods. Beamline 4B8 is optimized for these two kinds of spectroscopy to make efficient use of this wavelength range. To keep the measurement integrity, the range up to 360 nm is covered. Instrumentation for these two methods developed at 4B8 is described, and performance tests for both beamline and instrumentation are presented, confirming the high capability of these two kinds of experiments.

2. Description and performance of beamline 4B8

2.1. Brief description of the beamline

Both spectroscopy methods need high flux while CD requires a small flux density at the sample position to prevent irradiation damage to biomacromolecules. Low stray light levels are also essential for CD measurements, which require, however, a moderate resolution and wavelengths generally

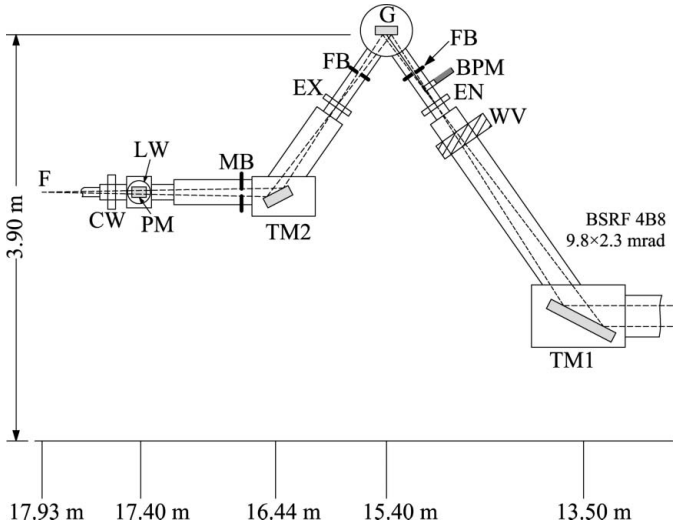

Figure 1
Layout of beamline 4B8. TM1, first toroidal mirror; WV, LiF window valve; EN, entrance slit; FB, fixed baffle; G, grating; EX, exit slit; TM2, second toroidal mirror; MB, movable baffle; PM, plane mirror; LW, LiF window; CW, CaF_2 window; F, focal point.

down to around 170 nm. Fluorescence measurements require excitation down to lower wavelengths (<140 nm).

The beamline design is described in detail elsewhere (Tao *et al.*, 2007). As shown in Fig. 1, the beamline mainly consists of a first toroidal mirror, lithium fluoride (LiF) window valve, Seya monochromator, second toroidal mirror, plane mirror and optical end-windows. The first toroidal mirror deflects the beam upwards at 62.5° incidence and focuses it vertically at the entrance slit. With the window valve closed it allows the part of the beamline behind this valve to be installed at atmospheric pressure with the beam on, providing considerable flexibility for installation and alignment of the beamline. The second toroidal mirror redirects the beam horizontally and focuses it at the sample position. By moving the plane mirror, the beam can be switched quickly into a different branch, for CD or fluorescence measurement. The LiF window is selected for the fluorescence chamber and the calcium fluoride (CaF_2) window for the CD chamber, since the LiF window reaches the lower cut-off wavelength as required by fluorescence measurements, while CD is recorded generally down to 170 nm at present and the CaF_2 window is also more chemically stable.

In addition, Beijing Synchrotron Radiation Facility (BSRF) is a parasitic light source, sharing the storage ring with the Beijing Electron Positron Collider (BEPC). In dedicated synchrotron mode the storage ring runs at 2.5 GeV with a peak beam current of 250 mA. In high-energy mode the energy is 1.89 GeV and the present peak current is 550 mA.

2.2. Assessment of beamline performance

The flux is illustrated in Fig. 2; its magnitude is $\sim 10^{11}$ photons s^{-1} with the peak wavelength located at $\sim$180 nm. The flux is estimated from the current of a photodiode (UVG-100; IRD). The distribution curve is obtained by recording the fluorescence of sodium salicylate, the fluorescence emission efficiency of which is constant in this range.

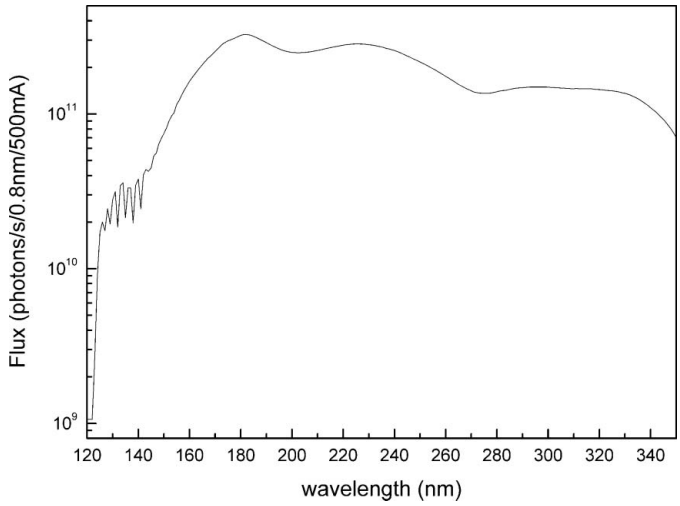

Figure 2
Photon flux at the CD sample position. The CD chamber is purged with nitrogen. The multiple peaks around 140 nm are from nitrogen absorption.

The beamline performance was evaluated using a series of reference samples (Starna). Wavelength calibration was realised using the holmium solution reference with characteristic absorption peaks between 240 and 290 nm (Fig. 3). Reproducibility of wavelength accuracy has been proven to be well kept to within 0.1 nm for a long-term operation.

The spectral resolution was determined using toluene in hexane reference solution using two slit widths (Fig. 4). The resolution was calculated using the absorbance ratio of the peak maxima to the minima. The stray light level was determined using a reference salt solution (Fig. 5). Below 200 nm the level is 0.06% which is adequate for SRCD measurements. The beamline parameters are summarized in Table 1.

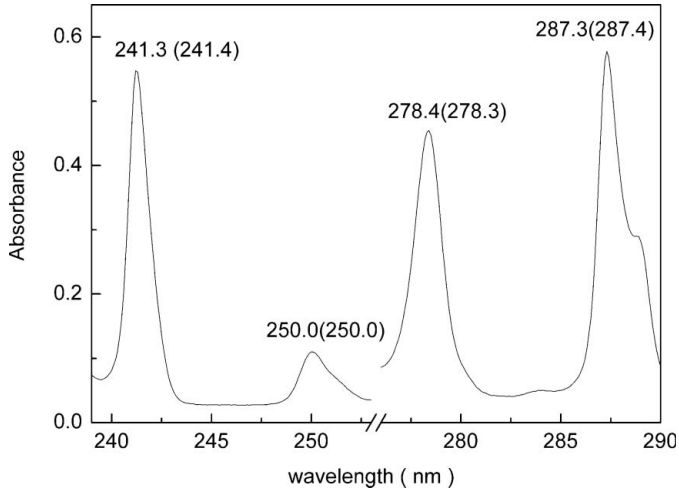

Figure 3
Wavelength calibration using the reference holmium oxide solution at a bandwidth of 0.75 nm with the reference values in brackets.

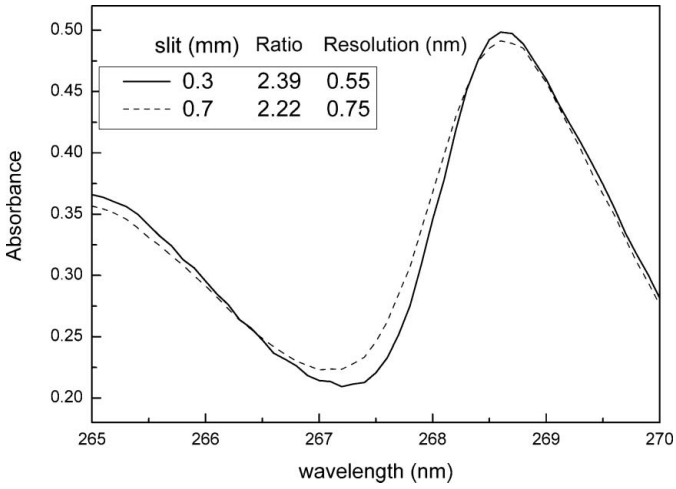

Figure 4
Spectral resolution determination using the reference toluene in hexane solution. The peak ratio of the maximum to the minimum absorbance measures the resolution.

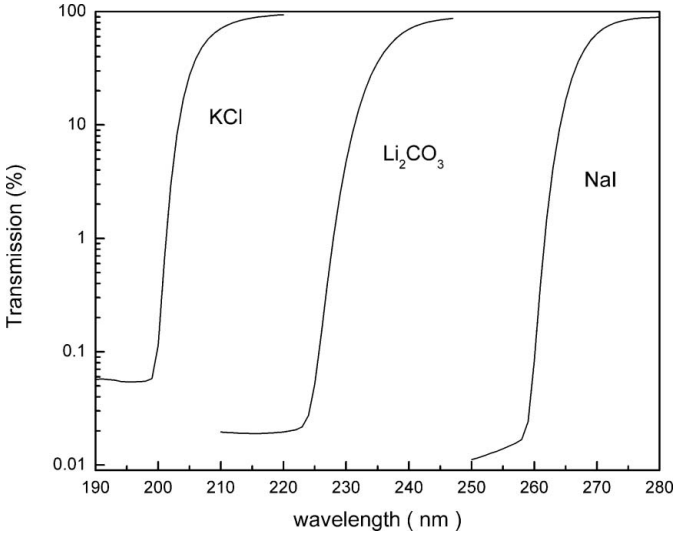

Figure 5
Stray light level assessment determined by the transmissions of the different reference salt solutions.

3. CD spectroscopy development

3.1. CD instrumentation

CD is the differential absorption between circular left- and right-polarized light by chiral biomolecules. A photoelastic modulator (PEM90, CaF_2 crystal optical head; Hinds Instruments) is used to convert linear polarized light into left- and right-circularly polarized light at 50 kHz. Circular polarization is dependent on linear polarization, so a Seramont polarizer (B-Halle GmbH) is installed in front of the PEM to maintain a high linear polarization. The PEM was calibrated by setting the retardation to make the CD signal maximized at 192.5 nm for reference sample (1*s*)-(+)-10-camphorsulphonic acid (CSA) (Oakberg *et al.*, 2000).

CD detection is schematically shown in Fig. 6. The alternately changed circularly polarized light passes through the sample and reaches a PMT detector (R6836 solar blind photomultiplier tube; Hamamatsu). The signal is amplified by a preamplifier (A1H; Electron Tubes) with a bandwidth of 150 kHz to eliminate the high-frequency noise. The amplified signal is then separated into AC and DC components by a signal-processing unit (SCU100; Hinds Instruments). The DC component feeds back to a home-made high-voltage servo controller (HT servo), which keeps the DC component constant during the spectroscopy scan by adjusting the high voltage (HT) applied on the PMT. The AC component is input into a lock-in amplifier (Model7265; Signal Recovery) to pick up the CD signal. The CD, DC, high voltage and beam current signals are all collected.

Table 1
Summary of the beamline 4B8 parameters.

Acceptance	9.8 mrad × 2.3 mrad
Wavelength range	120–360 nm (10–3.5 eV)
Bandwidth	>0.55 nm
Wavelength repeatability	<0.1 nm
Flux at sample	$\sim 10^{11}$ photons s^{-1} (500 mA)$^{-1}$
Spot size at sample	1 mm × 1 mm for fluorescence; variable from 2 mm × 1.5 mm to 8 mm × 2 mm for CD
Stray light level	~0.06%

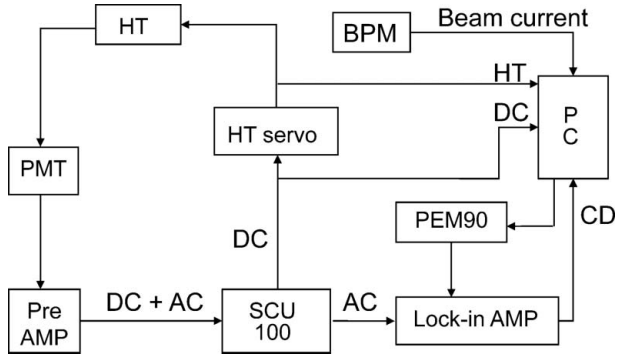

Figure 6
Block diagram of 4B8 CD detection instrumentation: PMT high-voltage control servo, signal processing and data-acquisition system.

During the CD scan the absorption can be recorded simultaneously using the established method of the transmission signal being combined with the recorded high voltage, the PMT gain and the beam current to restore the absorption (Sutherland, 1996).

Instead of evacuating the chamber, the SRCD sample chamber is purged with nitrogen to make the measurement convenient: high-purity dry gas from the evaporation of liquid nitrogen removes oxygen in the optical path in the instrument. The sample temperature is controlled by a Peltier temperature controller.

To detect membrane proteins and other turbid samples, the sample has to be close to the detector to reach a large acceptance angle, thus minimizing the artefact associated with light scattering from these samples (Wallace *et al.*, 2003). The distance from sample to detector surface is variable at beamline 4B8 and can be as small as 10 mm to reach the required 90° acceptance.

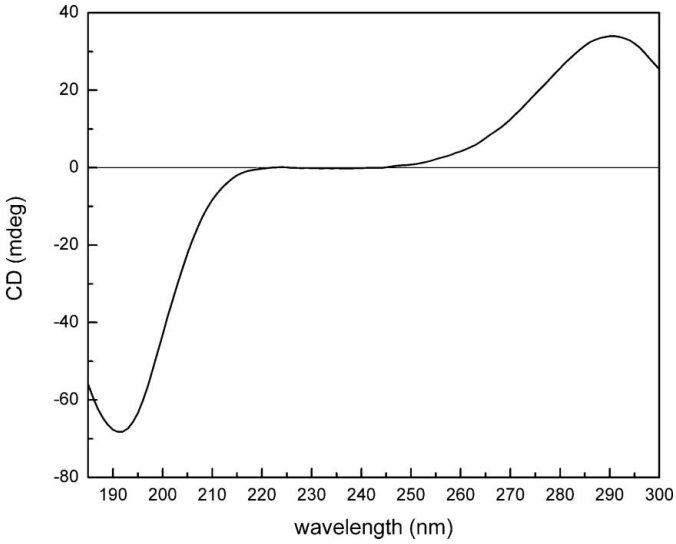

Figure 7
CD spectrum of CSA, 1 mg ml^{-1} in 1 mm-pathlength cell. The ratio of the two band maxima at 192.5 nm and 290.5 nm is 1.98.

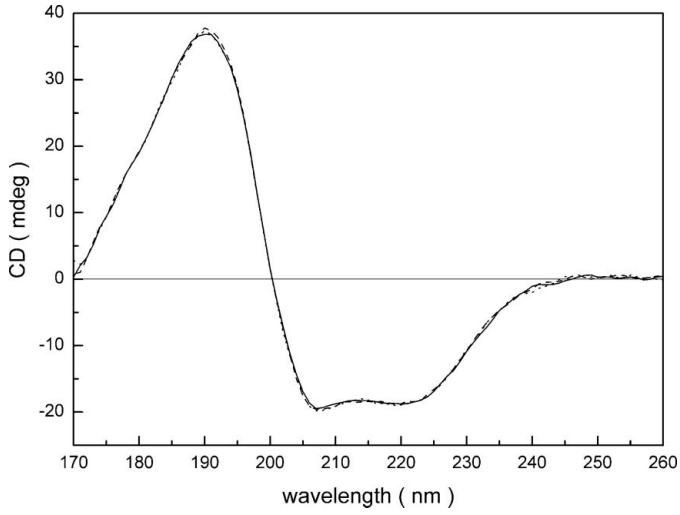

Figure 9
Plot of three consecutive scans of HSA; protein concentration ~7.5 mg ml^{-1}, 0.01 mm cell.

3.2. Performance of CD instrumentation

CSA is commonly used as a calibration sample for CD spectrometers. As shown in Fig. 7, the ratio of two characteristic peaks ($\theta_{192.5\text{nm}}$ to $\theta_{290.5\text{nm}}$) is 1.98 ± 0.01, which demonstrates that the instrumentation has been well calibrated and the stray light level well controlled (Miles *et al.*, 2003). All of the CD data are processed using the *CDtool* program (Lees *et al.*, 2004).

Beamline 4B8 provides routine CD measurements down to as low as 172 nm for aqueous solutions, using a 0.01 mm-pathlength quartz cell (124; Hellma). When the CaF_2 cell is used, shorter wavelengths can be realised below 170 nm (Fig. 8).

UV–VUV irradiation effects on biomolecule denaturation have initiated concern for SRCD measurements (Wien *et al.*, 2005). It was found that there is a threshold of the flux density for denaturation (Miles *et al.*, 2008). Human serum albumin (HSA) is generally used as an irradiation denaturation indicator as it is vulnerable to UV–VUV irradiation. At the dedicated operation mode with a beam current of ~200 mA, multiple scans of HSA show that the irradiation damage is negligible with a 4 mm × 1.5 mm irradiation area (Fig. 9). However, the irradiation damage is apparent in the parasitic mode when the beam current exceeds 400 mA. The adverse effect can be minimized when the sample is moved downstream to enlarge the spot size up to 8 mm × 2 mm and concomitantly decrease the flux density.

The sample temperature can be controlled between 275 and 368 K. The melting curve of myoglobin is shown in Fig. 10.

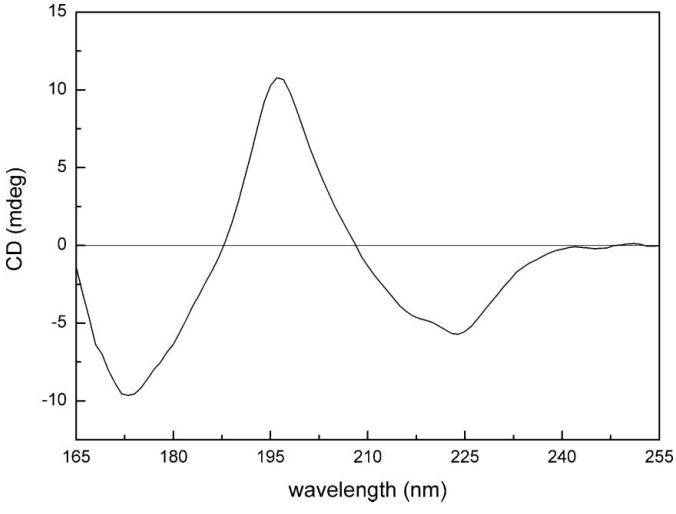

Figure 8
CD spectrum of concanavalin IV protein; protein concentration ~7 mg ml^{-1}, using 0.01 mm CaF_2 cell and D_2O as solvent.

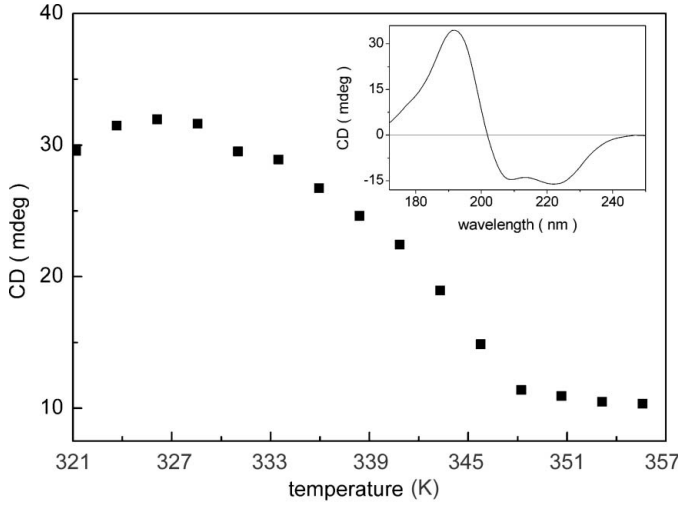

Figure 10
Thermal denaturation curve of myoglobin as a function of temperature, monitoring at 192 nm. Inset: CD spectrum of myoglobin from equine skeletal muscle; protein concentration ~7 mg ml^{-1}, 0.01 mm cell.

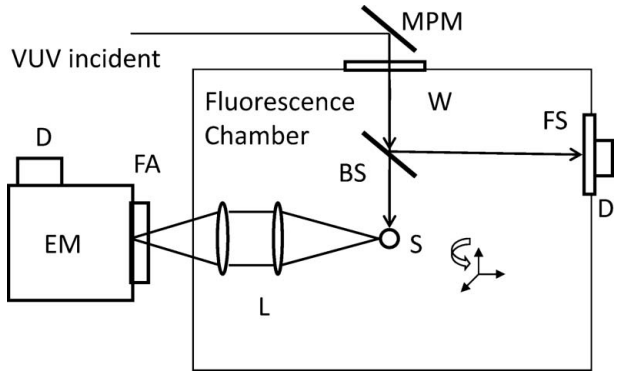

Figure 11
Optical layout of fluorescence instrumentation. BS: beam splitter; MPM, movable plane mirror; D, detector; EM, emission monochromator; FA, filter assembly; FS, fluorescence screen; L, lenses; S, sample; W, LiF window.

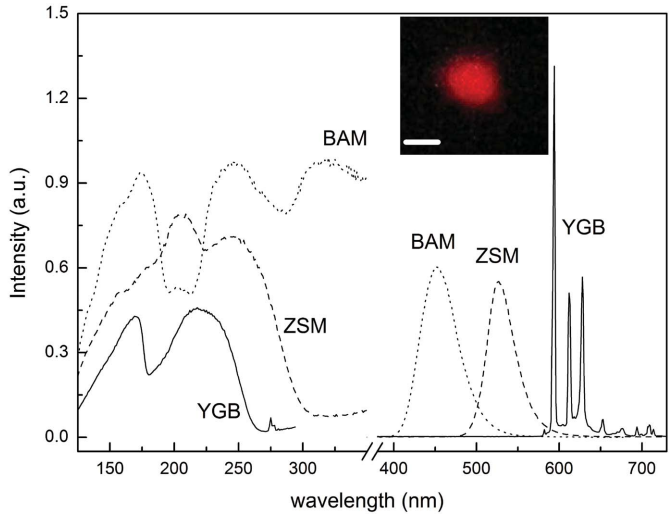

Figure 12
Photoluminescence of red, green and blue emitting phosphors. Solid line: $(Y,Gd)BO_3:Eu^{3+}$ (YGB), red light; dashed line, $Zn_2SiO_4:Mn^{2+}$ (ZSM), green light; dotted line, $BaMgAl_{10}O_{17}:Eu^{2+}$ (BAM), blue light. Left: excitation spectra with emission wavelength at 594 nm, 526 nm and 452 nm for YGB, ZSM and BAM, respectively. Right: emission spectra, all excited at 172 nm. Inset: the luminescence image of YGB with 1 mm scale bar.

4. Fluorescence spectroscopy development

4.1. Fluorescence instrumentation

The optical layout for VUV excited photoluminescence measurement is shown schematically in Fig. 11. For fluorescence measurements the plane mirror is moved in to switch the beam horizontally by 95° into the fluorescence chamber though the LiF optical window. A LiF beam splitter then reflects part of the beam to excite a sodium salicylate fluorescence screen to monitor the change of the incident flux, while the transmitted beam is focused at the sample. A sample holder can hold up to seven samples. A cryostat head with the sample holder is installed on a manipulator (MB1504; McAllister), which is used to adjust, optimize and restore the sample position. The fluorescence detection part is arranged perpendicular to the excitation beam. The fluorescence is collected and focused by two lenses and projected onto the entrance slit of a fluorescence monochromator (SP308; Acton), which holds three gratings covering the range from 190 to 1700 nm with spectral resolution of 0.2 nm. A motorized filter shifter provides a choice of eight long-pass optical filters. To avoid anisotropy effects, a polarizer at the magic angle can be installed in the emission path.

The fluorescence signals are detected by the photon-counting heads (H6241; Hamamatsu), the output TTL pulses of which are input into the counter module (974; ORTEC). The sample signal is calibrated from the sodium salicylate signal. The reflectance is required to determine the quantum efficiency. With a fluorescent screen inserted between the sample and the collecting lens, the sample reflectance can be obtained by detecting the fluorescence excited by the UV–VUV reflection (Justel *et al.*, 2001). A CCD camera is mounted facing the sample surface to record the fluorescence image. The chamber is evacuated using a turbo pump (Turbo70; Varian). Fig. 12 shows a series of VUV excitation and emission spectra for the typical commercial red (YGB), green (ZSM) and blue (BAM) emitting phosphors.

Remote access has been realised for fluorescence measurements. A remote desktop (Radmin; FASCO) runs on the user's home computer and displays the beamline 4B8 desktop. With the aid of instrumentation automation, users are able to complete the measurement as if they were at beamline 4B8 by choosing a sample, optimizing the sample position, selecting a filter, controlling the sample temperature (down to 14 K), collecting data and finally transferring data.

4.2. Fluorescence lifetime measurement

Fluorescence lifetime detection is essential to fluorescence study. Synchrotron radiation has been the favourable excitation source for fluorescence lifetime measurement owing to its merits of short pulse, high repetition frequency and wide tunable wavelength range. The pulse duration is 150 ps with pulse interval 800 ns under single-bunch mode at the BSRF. The fluorescence lifetime is measured in the time domain by using the time-correlated single-photon-counting (TCSPC) method. The reversed start–stop technique is employed such that the pulse signal from the sample is used to start a time-to-amplitude converter (TAC) and the excitation reference pulse is used to stop the TAC.

As shown in Fig. 13, the sample pulse is detected by a fast PMT (XP2020Q; Photonis) and discriminated by a constant fraction discriminator (583; ORTEC) before input into the TAC (576; ORTEC). It can also be detected by a single-photon-counting unit (H7421-50; Hamamatsu), the output TTL signal of which can be input directly into the TAC. The detectors are mounted at the exit slit port of the emission monochromator. By detecting the visible reflection from the entrance slit of the beamline the excitation reference pulse is obtained using another PMT (XP2020). The signal is then discriminated and delayed before input to the TAC. The TAC output is input into a multichannel analyzer (Trump MCA card; ORTEC) to restore the decay curve. To avoid pulse pile-

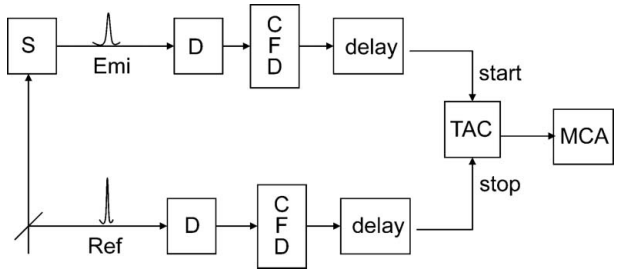

Figure 13
Block diagram of the TCSPC set-up. Ref, synchrotron radiation reference pulse; S, sample; Emi, sample emission; D, detector; CFD, constant fraction discriminator; TAC, time-to-amplitude converter; MCA, multi-channel analyzer.

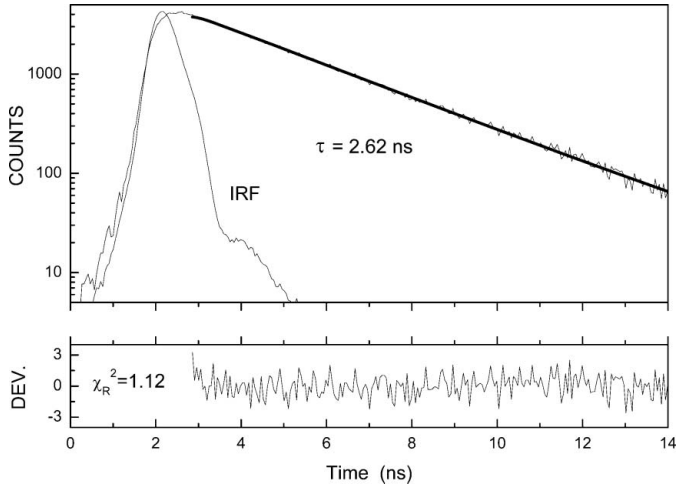

Figure 14
Fluorescence decay curve of *N*-acetyl-L-tryptophanamide (NATA) in water, 280 nm excitation and 350 nm emission. Bold line, fitting result. IRF, instrumentation response function.

up, the counting rate is kept below 1% of the repetition frequency.

A compound of known lifetime was used to test the capability of the instrumentation. An intensity decay curve of *N*-acetyl-L-tryptophanamide (NATA) is shown in Fig. 14. The measured lifetime (2.62 $\pm$ 0.35 ns) agrees with the reported value (Lakowicz, 1983). The instrumentation response function (IRF) was measured by detecting scattering of the excitation pulse.

5. Summary and future developments

Instrumentation at beamline 4B8 has been developed for both CD and fluorescence spectroscopy. It has been applied for VUV fluorescence studies in fields such as the new white-emitting phosphors (Zhong *et al.*, 2008) and the quantum cutting emission study (Tian *et al.*, 2008). Because the users are geographically dispersed, most fluorescence studies have been carried out through remote access. Also, SRCD has been used in different fields such as detecting trace heavy metal ions from DNA–carbon nanotube interaction (Gao *et al.*, 2008), combining crystallography and SRCD to examine interactions of disease-related proteins (Liu *et al.*, 2009) and providing evidence of the origin of the chiral asymmetry of the synthesized amino acid (Burkov *et al.*, 2008).

As a next step, the time-resolved methods will be focused on. In order to study protein folding dynamics, a pump–probe instrumentation set-up is underway such that a laser-induced temperature jump is used to pump the sample, with both CD and middle-IR (MIR) absorption measurements as probes. The latter will be used not only as a measurement of the temperature change but also as a complementary probe for protein folding (Dyer *et al.*, 1998). MIR will cover the nanosecond to microsecond dynamics while CD will focus on the millisecond range. Heating will be achieved using output from a Nd:YAG laser incorporating optical parametric oscillator devices.

For fluorescence lifetime measurements, a hybrid fill pattern will be commissioned such that a single bunch is inserted into a large gap among multiple bunches to keep the ring current high enough for steady-state experiments, and in the meantime the single bunch is used for time-resolved measurements. The timing signal from the BEPC master oscillator will be used to select this single bunch.

Remote access has been well used but sometimes it has suffered from low internet speeds that cause operation delays in remote desktops. The current control program was developed using *Labview*. By utilizing the TCP/IP communication module inside *Labview*, the control code will be rewritten and will replace the present remote desktop method to provide a quicker and safer access. Remote access to the CD measurement is also feasible with the development of the high-throughput CD technique.

We gratefully acknowledge support from the National Natural Science Foundation of China (10635060 and 20871116) and the Innovation Fund of Institute of High Energy Physics (IHEP). We thank Professor Hongbin Liang (Sun Yat-sen University) for providing phosphors. We are grateful to Professor Baoyi Wang and Dr Zhiming Zhang (IHEP) who gave support in setting up the TCSPC instrumentation. We also thank Zhuoxian Wang (Wuhan University) for his considerable help in analysis of fluorescence lifetime data.

References

Burkov, V. I., Goncharova, L. A., Gusev, G. A., Kobayashi, K., Moiseenko, E. V., Poluhina, N. G., Saito, T., Tsarev, V. A., Xu, J. H. & Zhang, G. B. (2008). *Orig. Life Evol. Biospheres*, **38**, 155–163.
Clarke, D. T. & Jones, G. (2004). *J. Synchrotron Rad.* **11**, 142–149.
Dicko, C., Knight, D., Kenney, J. M. & Vollrath, F. (2004). *Biomacromolecules*, **5**, 758–767.
Dyer, R. B., Gai, F. & Woodruff, W. H. (1998). *Acc. Chem. Res.* **31**, 709–716.
Gao, X., Xing, G., Yang, Y., Shi, X., Liu, R., Chu, W., Jing, L., Zhao, F., Ye, C., Yuan, H., Fang, X., Wang, C. & Zhao, Y. (2008). *J. Am. Chem. Soc.* **130**, 9190–9192.
Justel, T., Krupa, J. & Wiechert, D. U. (2001). *J. Lumin.* **93**, 179–189.
Lakowicz, J. R. (1983). *Principles of Fluorescence Spectroscopy*, edited by J. R. Lakowicz, pp. 427–485. New York: Plenum Press.
Lee, T., Luo, L., Cheng, B. M., Diau, E. & Chen, T. M. (2008). *Appl. Phys. Lett.* **92**, 081106.

Lees, J. G., Smith, B. R., Wien, F., Miles, A. J. & Wallace, B. A. (2004). *Anal. Biochem.* **332**, 285–289.
Lin, H., Liang, H., Han, B., Zhong, J., Su, Q., Dorenbos, P., Birowosuto, M. D., Zhang, G., Fu, Y. & Wu, W. (2007). *Phys. Rev. B*, **76**, 035117.
Liu, H., Peng, X., Zhao, F., Zhang, G., Tao, Y., Luo, Z., Li, Y., Teng, M., Li, X. & Wei, S. (2009). *Biochem. Biophys. Res. Commun.* **379**, 1120–1125.
Matsuo, K., Fukuyama, T., Yonehara, R., Namatame, H., Taniguchi, M. & Gekko, K. (2005). *J. Electron Spectrosc. Relat. Phenom.* **144**, 1023–1025.
Miles, A. J., Janes, R. W., Brown, A., Clarke, D. T., Sutherland, J. C., Tao, Y., Wallace, B. A. & Hoffmann, S. V. (2008). *J. Synchrotron Rad.* **15**, 420–422.
Miles, A. J. & Wallace, B. A. (2006). *Chem. Soc. Rev.* **35**, 39–51.
Miles, A. J., Wien, F., Lees, J., Rodger, A., Janes, R. W. & Wallace, B. A. (2003). *Spectroscopy*, **17**, 653–661.
Mirona, S., Refregiersa, M., Gilles, A. & Maurizot, J. (2005). *Biochim. Biophys. Acta*, **1724**, 425–431.
Oakberg, T. C., Trunk, J. & Sutherland, J. C. (2000). *Proc. SPIE*, **4133**, 101–111.
Sedhain, A., Tahtamouni, T. M. A., Li, J., Lin, J. Y. & Jiang, H. X. (2008). *Appl. Phys. Lett.* **93**, 141104.
Sutherland, J. (1996). *Circular Dichroism and the Conformational Analysis of Biomolecules*, edited by G. Fasman, pp. 599–634. New York, London: Plenum Press.
Sutherland, J. (2002). *Proc. SPIE*, **4625**, 126–136.
Tao, Y., Huang, Y., Qian, H., Yan, Y., Xu, J. & Zheng, H. (2007). *AIP Conf. Proc.* **879**, 555–558.
Tian, Z., Liang, H. B., Han, B., Su, Q., Tao, Y., Zhang, G. & Fu, Y. (2008). *J. Phys. Chem. C*, **112**, 12524–12529.
Wallace, B. A., Lee, S. J. G., Orry, A. J. W., Lobley, A. & Janes, R. W. (2003). *Protein Sci.* **12**, 875–884.
Wegh, R. T., Donker, H., Oskam, K. D. & Meijerink, A. (1999). *Science*, **283**, 663–666.
Wien, F., Miles, A. J., Lees, J. G., Vrønning Hoffmann, S. & Wallace, B. A. (2005). *J. Synchrotron Rad.* **12**, 517–523.
Yagi-Watanabe, K., Tanaka, M., Kaneko, F. & Nakagawa, K. (2007). *Rev. Sci. Instrum.* **78**, 123106.
Zhong, J. P., Liang, H. B., Han, B., Tian, Z., Su, Q. & Tao, Y. (2008). *Opt. Express*, **16**, 7510–7518.
Zimmerer, G. (2007). *Radiat. Meas.* **42**, 859–864.